Journal of Research in Science and Engineering (JRSE)
ISSN: 1656-1996 Volume-7, Issue-4, April 2025
DOI: 10.53469/jrse.2025.07(04).08

Kinetic Characteristics Analysis of Hydraulic Boom of In-Cabin Palletizer Considering Working Condition Parameters

Mingtao Liu, Youshuang Jin*, Gang Chen

Tianjin University of Science and Technology, School of Mechanical Engineering, Tianjin 300450, China
**Correspondence Author, 171232289@qq.com*

Abstract: ***To address collision risks and spatial limitations of hydraulic booms in in-cabin palletizers operating within confined cargo holds, this study proposes a safety framework integrating kinematic analysis and collision detection. The method constructs a kinematic model mapping hydraulic cylinder displacements to boom rotation angles, incorporating geometric constraints from cylinder parameters and boom cross-sectional dimensions. Forward/inverse kinematic solutions generate motion trajectories compliant with workspace boundaries. Obstacle geometric models embedded in the kinematic framework enable real-time collision detection and automatic safety braking during operation. Monte Carlo-based stochastic sampling quantifies the boom's reachable workspace in dynamic cargo stacking scenarios. Point-cloud distance field visualization reveals spatial relationships with obstacles, providing intuitive collision risk assessments. Experimental validation confirms the method's effectiveness in evaluating motion feasibility under complex loading conditions, offering theoretical support for scenario-specific system adaptation and environmental optimization. This research enhances in-cabin logistics automation reliability by addressing constrained-space motion planning and dynamic load compensation. The proposed approach ensures safe operation while improving workspace utilization compared to traditional methods.***

Keywords: Hydraulic, Collision detection, Kinematics, Work space.

1. Introduction

Ports serve as critical nodes in the integrated transportation chain and are vital for enhancing regional economic competitiveness and driving regional development [1-3]. The efficiency of cargo handling at docks is a key factor in improving port transportation capacity, with in-cabin operations representing the starting point of the entire dock workflow. Optimizing the mechanical performance of in-cabin machinery to meet production requirements remains a longstanding and evolving research topic.

In-cabin palletizers are medium-to-heavy-duty loading / unloading machinery commonly operating in the cargo holds of bulk cargo ships. They are widely applied to handle various cargos on cargo ships, such as cold-rolled coils, steel plates, and wire rods. The boom installed on the palletizer is its core mechanical structure. During operation, apart from its own gravity, the boom bears multiple complex loads—including dynamic cargo loads and inertial impact loads. Issues like boom sinking, downward deflection, lateral bending, and even web plate wavy deformation or fracture often occur. Meanwhile, due to the narrow operational space in cargo holds and changes in cargo stacking, the boom's operational space is frequently restricted. Since the reachable range of hydraulic cylinders, boom cross-sectional dimensions, and in-cabin operational space constraints must be considered, the boom's motion characteristics differ from both traditional high-speed lightweight manipulators and low-speed heavy-duty configuration equipment. Therefore, accurately analyzing the motion characteristics of the in-cabin palletizer's boom is of significant reference value for enhancing the reliability of in-cabin logistics automation systems.

Currently, research on kinematics modeling, motion simulation, and workspace analysis for high-speed light-load manipulators is already quite comprehensive. However, studies on the kinematics of in-cabin machinery are relatively limited. For instance, Liu Yan et al. conducted design research on heavy-load assembly robots in spatial cabins. They addressed the contradiction between spatial constraints and load-bearing via innovative mechanical structures, optimizing the robot's posture adjustment accuracy and motion stability in narrow spaces [4]. Literature performed kinematics modeling for artillery robotic arms, calculating motion variables of each arm and joint within the confined space of artillery channels, significantly enhancing the motion flexibility of traditional excavation equipment in confined spaces [5]. Literature proposed a self-reconfigurable spatial robotic arm system based on telescopic rods, analyzed and simulated telescopic rod mechanism parameters and layouts, and conducted motion planning simulation for target working conditions in narrow spaces. Results show that the cross-sectional telescopic design can improve the flexibility of the robotic arm system [6].

This paper takes into account kinematic pair dimension parameters, boom cross-sectional parameters, and in-cabin space limitation factors. Starting from the basic structure and working principle of the palletizer boom, it deduces the geometric relationships among components, establishes a forward kinematics model for the series-connected boom equivalent mechanism, and derives the mapping relationship between hydraulic cylinder displacement and boom rotation angle. Furthermore, the Monte Carlo method is employed to analyze the motion space of the hydraulic boom under the effect of cargo stacks, offering theoretical support for the subsequent design of the actual mechanical structure of the hydraulic boom and the determination of operational parameters.

2. Forward Kinematic Analysis of the Boom

2.1 Coordinate System Establishment for the Boom

The boom structure consists of a box-shaped configuration with a two-section folding boom combined with a single telescopic stage, actuated by three sets of drive hydraulic cylinders. This design enables complex motions such as load-bearing amplitude variation, closely resembling the structure of a manipulator with arms, joints, and an end-effector. Among coordinate system establishment methods, the standard Denavit-Hartenberg (DH) model has been widely adopted [7]. However, with increasing complexity in manipulator structures and rising precision requirements, modified DH models have gained prevalence. This study employs the modified Denavit-Hartenberg (MD-H) method to develop the forward kinematic model of the manipulator [8].

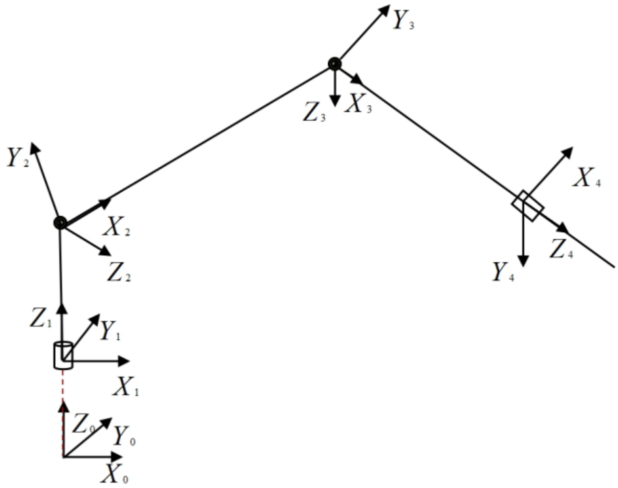

Figure 1: The DH coordinate system of the boom

For the hydraulic boom under study, the corresponding coordinate system was established using the MD-H method, as shown in Figure 1. The MD-H parameters of the boom are listed in Table 1.

Table 1: Nominal values of MDH parameters of the boom

Joint Number	Link Twist Angle α_{i-1}/(°)	Link Length α_{i-1}/(°)	Link Offset d_i/(mm)	Joint Angle θ_i/(°)
1	0	0	2	0
2	-90	0	0	90
3	0	-4.5	0	0
4	90	0	d_4	0

2.2 Forward Kinematic Solution of the Boom

Based on the established MD-H coordinate system and the MD-H parameter table of the actual hydraulic manipulator joint dimensions, the homogeneous transformation matrix for each joint can be calculated using the following formula (1):

$$ {}^{i-1}_{i}T = \begin{bmatrix} c\theta_i & -s\,\theta_i & 0 & \alpha_{i-1} \\ s\,\theta_i\,c\alpha_{i-1} & c\theta_i c\alpha_{i-1} & -s\,\alpha_{i-1} & -s\,\alpha_{i-1}\,d_i \\ s\,\theta_i\,s\,\alpha_{i-1} & c\theta_i\,s\,\alpha_{i-1} & c\alpha_{i-1} & c\alpha_{i-1}d_i \\ 0 & 0 & 0 & 1 \end{bmatrix} \quad (1) $$

The transformation matrix of the boom end is obtained by multiplying the homogeneous transformation matrices of each joint, as shown in Formula (2):

$$ {}^{4}_{0}T = {}^{1}_{0}T\,{}^{2}_{1}T\,{}^{3}_{2}T\,{}^{4}_{3}T = \begin{bmatrix} n_x & o_x & a_x & p_x \\ n_y & o_y & a_y & p_y \\ n_z & o_z & a_z & p_z \\ 0 & 0 & 0 & 1 \end{bmatrix} \quad (2) $$

3. Inverse Kinematic Analysis of the Boom

Hydraulic cylinders, as the driving components of the boom, have displacement strokes that affect the overall design of boom hinges, joint rotation angles, and arm lengths. The inverse kinematic solution involves solving the transformation from the pose space to the joint rotation angles and hydraulic drive space. Inverse kinematic analysis can establish the relationship between joint rotation angles and hydraulic cylinder lengths under different postures. Based on the pose of the boom end coordinates $[x \quad y \quad z \quad \theta_w]$ in the base coordinate system, the corresponding joint variables and hydraulic cylinder lengths are solved, that is, $\{x \quad y \quad z \quad \theta_w\} \rightarrow \begin{Bmatrix} \{\theta_1, \theta_2, \theta_3, \theta_4\} \\ \{\lambda_1, \lambda_2, \lambda_3\} \end{Bmatrix}$ [9]. Methods for solving inverse kinematics usually include the algebraic method, geometric method, and iterative method [10]. The algebraic method requires a large amount of matrix operations, resulting in high computational complexity, while the convergence of the iterative method is difficult to guarantee. The hydraulic boom belongs to a 4-degree-of-freedom robotic arm. Given its simple structure and object characteristics, the geometric method is adopted.

Inverse kinematics solution approach [11]:

(1) Initialize the boom end pose vector $[x \quad y \quad z \quad \theta_w]$, and solve for θ_1

(2) Calculate the translated coordinates (x', y', z') of the boom end position in the base coordinate system

(3) Determine the position coordinates (x_3, y_3, z_3) of point O_3 in the new base coordinate system.

(4) Calculate α and β based on geometric relationships.

(5) Compute θ_2 and θ_3

Assume the position coordinate of the boom end in the coordinate system $O_4 - X_4Y_4Z_4$ is ${}^{4}R = [0 \quad 0 \quad 0 \quad 1]$, then its coordinate in the base coordinate system $O_0 - X_0Y_0Z_0$ is ${}^{0}R = {}^{4}_{0}T\,{}^{4}R$, from which the boom end position coordinates can be obtained:

$$ \begin{cases} x = d_4c_1c_{23} - a_2c_1s_2 \\ y = d_4(s_2s_3 + c_2c_3) - a_2c_2 + d_1 \\ z = d_4c_{23} + a_2s_2 + d_1 \end{cases} \quad (3) $$

During the lifting process, θ_1 and θ_4 often remain unchanged. Thus, the direction angle of the boom end is uniquely determined by $\theta_w = \theta_2 + \theta_3$, and the pose of the boom end is $[x \quad y \quad z \quad \theta_w]$.

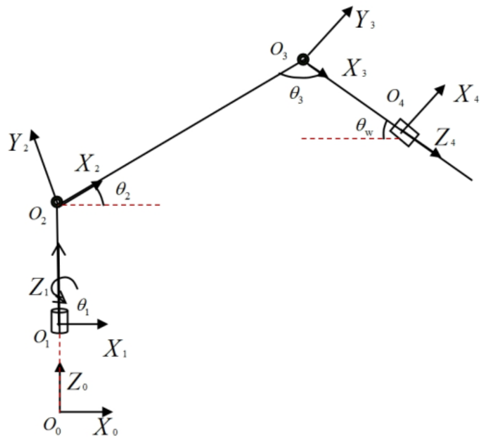

Figure 2: Schematic diagram of the linkage coordinate system

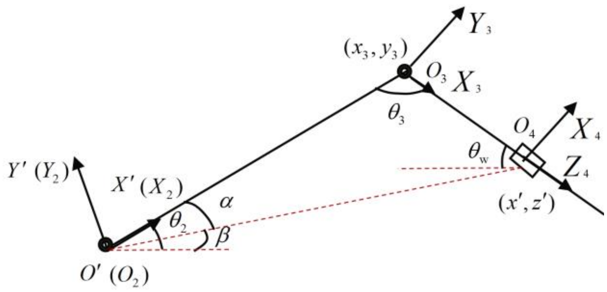

Figure 3: Schematic diagram of the computational geometry of the inverse kinematic solution

If the boom end pose is known as $[x \quad y \quad z \quad \theta_w]$, then according to Figure 2, the spatial geometric relationship is derived:

$$\theta_1 = arctan\left(\frac{y}{x}\right) \tag{4}$$

Translate the origin O_0 of the base coordinate system to O_2, and assume the translated base coordinate system is $O' - x'y'z'$. Then, based on the coordinates and angles shown in the following figure, it can be concluded that:

$$\begin{cases} x' = x \\ y' = y \\ z' = z - d_1 - d_2 \end{cases} \tag{5}$$

In the translated base coordinate system:

$$[x_3 \quad y_3 \quad z_3 \quad 1] = {}^1_0T\,{}^2_1T\,{}^3_2T[0 \quad 0 \quad 0 \quad 1]^T - [0 \quad 0 \quad d_1 + d_2 \quad 0]^T \tag{6}$$

Substituting Equations (1), (2), and (3) into Equation (9) yields:

$$\begin{cases} x_3 = -a_2 c\theta_1 s\theta_2 \\ y_3 = -a_2 s\theta_1 s\theta_2 \\ z_3 = -a_2 c\theta_2 - d_2 \end{cases} \tag{7}$$

From Equations (8), (10) and $\theta_w = \theta_2 + \theta_3$, we obtain:

$$\begin{cases} x_3 = x' - |O_3O_4| \cos\theta_1 \cos\theta_w \\ y_3 = y' - |O_3O_4| \sin\theta_1 \sin\theta_w \\ z_3 = |O_3O_4| \sin\theta_w \end{cases} \tag{8}$$

Here, $|O_2O_3|$ represents the length of the basic arm, and $|O_3O_4|$ denotes the length of the folding arm.

As shown in Figure 3, $|O_2O_4| = \sqrt{(x')^2 + (y')^2}$. Calculate α and β based on geometric relationships. These angles serve as crucial intermediate variables for establishing the connection between joint rotation angles and the end pose, with solutions derived as:

$$\begin{cases} \alpha = arccos\frac{|O_2O_3|^2 + |O_2O_4|^2 - |O_3O_4|^2}{2|O_2O_3||O_2O_4|} \\ \beta = arctan\left(\frac{z'}{x'}\right) \end{cases} \tag{9}$$

Calculate θ_2 and θ_3 based on the geometric relationships in Figure 4. The solution of these two joint angles is a key result of the inverse kinematic analysis. They directly determine the movement angles of each boom joint, thus determining the overall posture of the boom.

$$\begin{cases} \theta_2 = \alpha + \beta \\ \theta_3 = arccos\frac{|O_2O_3|^2 + |O_3O_4|^2 - |O_2O_4|^2}{2|O_2O_3||O_3O_4|} \end{cases} \tag{10}$$

4. Mapping Relationship between Hydraulic Cylinder Displacement and Boom Rotation Angle

4.1 Coordinate System Establishment of the Boom

Hydraulic cylinders serve as the actuators of the hydraulic boom. As shown in Figure 4, the length λ_n of the hydraulic cylinder determines the magnitude of each joint rotation angle θ_n . Obtaining joint rotation angles from the actuator mechanism's length is called forward transformation, while calculating the actuator mechanism's length from joint rotation angles is termed inverse transformation [12]. The length of the hydraulic cylinder can be represented by the distance between working hinges of the hydraulic arm, with specific solution steps as follows:

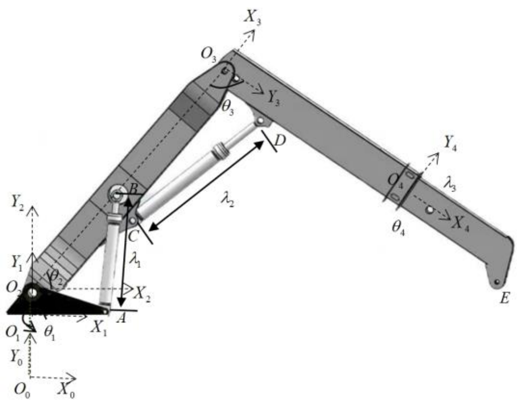

Figure 4: Schematic diagram of boom coordinates

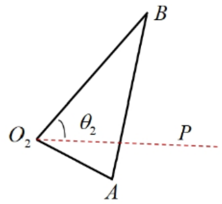

Figure 5: Schematic diagram of hydraulic cylinder and joint of basic arm

4.2 Relationship between the Length $\lambda_1$of the Basic Arm Hydraulic Cylinder and the Joint Variable θ_2

As shown in Figure 5, in triangle O_2AB:

$$\lambda_1 = |AB| = \sqrt{|O_2B|^2 + |O_2A|^2 - 2|O_2B||O_2A| \cos \angle AO_2B} \quad (11)$$

where O_2A and O_2B are known values:

$$\theta_2 = \angle AO_2B - \angle AO_2P = arccos\frac{|O_2B|^2+|O_2A|^2-\lambda_1{}^2}{2|O_2B||O_2A|} - \angle AO_1P \quad (12)$$

4.3 Relationship between the Length λ_2 of the Folding Arm Hydraulic Cylinder and the Joint Variable θ_3

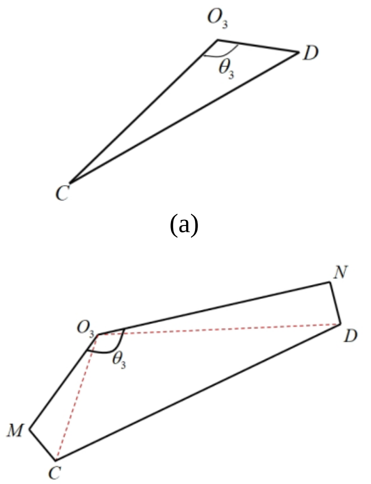

(a)

(b)

Figure 6: Schematic diagram of hydraulic cylinder and joint of the folding arm without considering the influence of cross section

4.3.1 Relationship between the Length λ_2 of the Folding - Arm Hydraulic Cylinder and the Joint Variable θ_3 without Considering Cross - Section Influence

As shown in Figure 6 (a), based on the geometric relationships in the figure:

$$\lambda_2 = |CD| = \sqrt{|O_3C|^2 + |O_3D|^2 - 2|O_3C||O_3D| \cos \angle CO_3D} \quad (13)$$

Where O_3C and O_3D are known, and $\theta_3 = \angle CO_3D$. Then it can be solved as:

$$\theta_3 = \angle CO_3D = arccos\frac{|O_3C|^2+|O_3D|^2-\lambda_2{}^2}{2|O_3C||O_3D|} \quad (14)$$

4.3.2 Relationship between the Length λ_2 of the Folding Arm Hydraulic Cylinder and the Joint Variable θ_3 Considering Cross - Section Influence

Figure 6 (b) shows the boom cross - sections CM, DN, and the known distances between hinge points MO3, NO3. Based on the geometric relationships in the figure:

$$|CO_3| = \sqrt{|CM|^2 + |MO_3|^2} \quad (15)$$

$$\angle CO_3M = arctan\frac{|CM|}{|MO_3|} \quad (16)$$

$$|DO_3| = \sqrt{|DN|^2 + |NO_3|^2} \quad (17)$$

$$\angle DO_3N = arctan\frac{|DN|}{|NO_3|} \quad (18)$$

$$\lambda_2 = |CD| = \sqrt{|CO_3|^2 + |DO_3|^2 - 2|CO_3||DO_3| \cos \angle CO_3D} \quad (19)$$

$$\angle CO_3D = arccos\frac{|CO_3|^2+|DO_3|^2-\lambda_2{}^2}{2|CO_3||DO_3|} \quad (20)$$

It can be solved that:

$$\theta_3 = \angle MO_3N = \angle CO_3M + \angle CO_3D + \angle DO_3N = arctan\frac{|CM|}{|MO_3|} + arccos\frac{|CO_3|^2+|DO_3|^2-\lambda_2{}^2}{2|CO_3||DO_3|} + arctan\frac{|DN|}{|NO_3|} \quad (21)$$

5. Workspace Solution of the Hydraulic Boom

The workspace of a robotic arm is determined by the movement range of its joints. Through inverse solution, the target position in the task space can be mapped to the joint space, enabling the robotic arm to complete various tasks as efficiently as possible within its reachable workspace [13]. As a key indicator of in-cabin palletizers, analyzing the workspace of hydraulic booms mainly aims to verify whether the boom meets the narrow operation space of the ship cabin during design and adapts to cargo stack changes.

The internal operation environment of the ship cabin is a typical limited-space scenario. Its complex structure and limited space dimensions severely restrict the movement of heavy-duty robotic arms. The ship cabin's interior is equipped with various supporting structures, pipelines, and installed ventilation devices. When the in-cabin palletizer operates, the robotic arm's movement is limited in multiple directions. For example, the height direction is restricted due to the ship's ceiling structure. This requires the robotic arm to adjust joint angles reasonably to complete tasks during high-altitude operations instead of moving freely like an open-space robotic arm. From a horizontal perspective, the supporting structures and fixed equipment in the cabin also divide the space, meaning the robotic arm's movement range in both translation and rotation is strictly limited.

The hydraulic boom is installed on the crawler chassis platform of the palletizer to lift steel plates, with its boom base joint 2m above the ground. Multiple cargo stacks are distributed in the cabin. By using boundary condition equations to describe the movement range limitations of the robotic arm's joints, and considering the position/shape of obstacles as well as the cross-sectional dimensions of the end effector, a geometric model of obstacles is established and incorporated into the kinematics model. Motion trajectories are then generated to ensure the robotic arm does not collide with obstacles during movement.

The Monte Carlo method is adopted to analyze the movement space of the hydraulic boom under cargo stack influence. By randomly generating a large number of sample points within the value range of each joint variable of the hydraulic boom, setting the robotic arm's dimension parameters, joint movement range, and assembly space boundary conditions, these sample points at the end position are converted into the end executor's position coordinates in the cartesian space through forward kinematics [14]. Points close to obstacles are filtered out. Finally, collision detection is repeated—

searching for positions in the reachable space that do not collide with obstacles in the given environment, and further considering tolerance compensation for re-collision detection, so as to more accurately determine the robot’s safe reachable space.

The end executor’s workspace point cloud map of the boom under cargo stack occlusion conditions and the theoretical workspace point cloud map without obstacles, obtained under the same conditions, are shown in Figure 7. The distance-based visualization intuitively demonstrates the corresponding relationship between the hydraulic boom’s different postures and obstacles. By evaluating the workspace connectivity and safety of the in-cabin palletizer’s movement, it is confirmed that the robotic arm avoids collisions in the workspace and reasonably plans movement paths through obstacle avoidance algorithms for cargo stack obstacles, ensuring the integrity of the boom and arm’s cross-sectional dimensions. The workspace point cloud circumvents obstacles to form avoidance areas, with some areas showing "air gaps" to reduce coverage, which is a direct manifestation of route optimization.

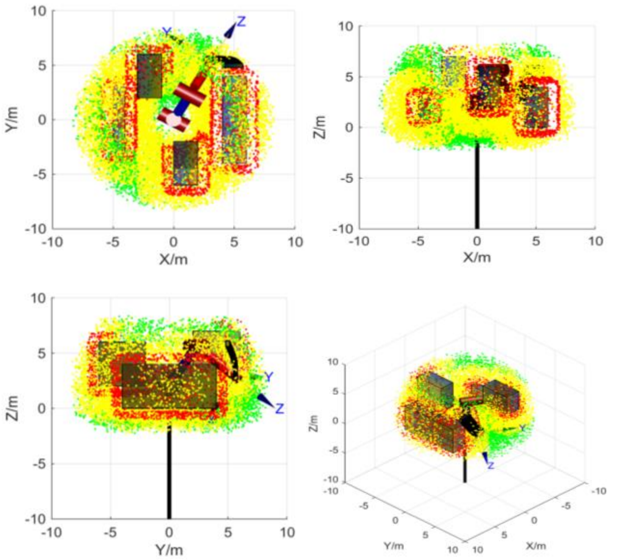

(a)Workspace diagram with obstacles

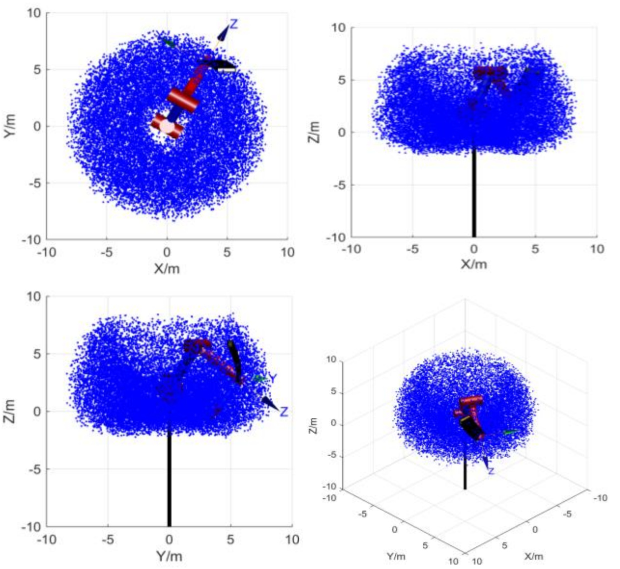

(b)Workspace diagram without obstacles

Figure 7: Point cloud diagram of hydraulic boom workspace

6. Conclusion

This paper considers the influence of hydraulic cylinder installation positions, movable spaces, and boom cross-sectional parameters in the hydraulic boom of large in-cabin palletizers. By analyzing the geometric relationships among components of the in-cabin palletizer’s working device, a mapping relationship between hydraulic cylinder displacement and boom rotation angle was established. Distance-based visualization intuitively displays the hydraulic boom’s positional relationship with obstacles at different positions, aiding in evaluating the motion feasibility and safety of the in-cabin palletizer to ensure collision-free movement. The obtained point cloud diagram exhibits a relatively dense, uniform, and compact distribution, confirming that the hydraulic boom’s joints meet the working-radius design requirements. Observing changes in reachable space and collision risks can provide a basis for selecting practical application scenarios and environmental modifications for in-cabin palletizers, ensuring stable operation in complex and dynamic real-world environments. However, further exploration of workspace-influencing factors is still needed. The cross-sections of boom members and their rotational-angle ranges significantly impact the robotic arm’s workspace, and optimizing these rotational ranges remains an ongoing challenge.

References

[1] Central Committee of the Communist Party of China and the State Council. Outline for Building a Transportation Power. People's Daily, September 20, 2019 (4).

[2] Mao, J. H. Accelerating the Establishment of a World-Class Strong Port and a World-Class Port Cluster. China Water Transport, 2020, 1: 2.

[3] Cui, J. R. Completion of the Tianjin Port Master Plan: Creating a "One Port, Nine Districts" Layout. Science & Technology of Ports, 2010, 9(53): 51–52.

[4] Liu, Y., Yi, W. M., Yao, J. T., et al. Design and Research of Heavy-Duty Posture-Adjusting Assembly Robots in Narrow Spaces. Chinese Journal of Mechanical Engineering, 2024, 35(2): 324–336.

[5] Jia, L. F., Ma, C. F., Liu, K. Workspace Analysis of Hard Rock Tunneling Machine’s Auxiliary Slag-Clearing Device Based on Monte Carlo Method. Journal of Mechanical Transmission, 2020, 44(4): 74–79.

[6] Wang, K., Liang, C. C, Lin, C. Y., et al. Research and Design of Space Manipulator System Based on Telescopic Arm. Applied Mechanics and Materials, 2017, 443: 508–517.

[7] Chen, G. M., Huang, W., Luo, M. Z., et al. Kinematic Analysis of Vehicle-Mounted Hydraulic Manipulator for Gravel Collection. Mechanical Research & Application, 2022, 35(5): 94–97.

[8] Peng, G. Y., Dong, H. B., Ma, B. Comparative Study on Kinematic Modeling of Two DH Models for Robots. Mechanical Research & Application, 2019, 32(6): 62–65.

[9] Zhang, D. Q. Research on Motion Control of Hydraulic Excavator Working Device. Ph.D. dissertation, Central South University, Changsha, China, 2006.

[10] Koivo, A. J., Thoma, M., Kocaoglan, E., et al. Modeling and Control of Excavator Dynamics During Digging

Operation. Journal of Aerospace Engineering, 1996, 9(2): 10–18.
[11] Li, B., Yan, J., Zeng, Y. H., et al. Kinematic Modeling and Analysis of Excavator Working Device. Journal of Mechanical Design, 2011, 28(10): 7–10.
[12] Deng, H. M., Pan, Z. K., Lin, X. W., et al. Vision Robot Hand-Eye Calibration Method Based on Circular Hole Calibration Plate. Machinery & Electronics, 2024, 42(2): 61–68.
[13] Guan, Y., Yokoi, K. Reachable Space Generation of a Humanoid Robot Using the Monte Carlo Method. In Proceedings of the 2006 IEEE/RSJ International Conference on Intelligent Robots and Systems (IROS 2006) (pp. 508–517). Beijing, China: IEEE, 2006.
[14] Liu, J. J., Peng, J. Q., Liu, X. H. Forward Kinematics Analysis and Simulation of a Serial-Parallel Hybrid 7-DOF Humanoid Manipulator Based on MATLAB. Journal of Mechanical Transmission, 2015, 39(7): 5.

Author Profile

Mingtao Liu (born in 1974), Female, Associate Professor, Ph.D. Research interests include Mechanism Science and Mechanical Transmission. Email: liumingtao@tust.edu.cn.